ISSN 0020-1685, Inorganic Materials, 2020, Vol. 56, No. 11, pp. 1106–1112. © Pleiades Publishing, Ltd., 2020.
Russian Text © The Author(s), 2020, published in Neorganicheskie Materialy, 2020, Vol. 56, No. 11, pp. 1168–1174.

Structure of $(ZrTi)_{0.5}(VCrFe(Ni_{0.9}Cu_{0.1}))_{0.5}$- and $(ZrTi)_{0.5}(VMoFeNi)_{0.5}$-Based Deuterides

M. A. Sobko[a], S. A. Lushnikov[a, *], V. N. Verbetsky[a], and S. S. Agafonov[b]

[a] *Moscow State University, Moscow, 119991 Russia*

[b] *Kurchatov Institute (National Research Centre), Moscow, 123182 Russia*

**e-mail: lushnikov@hydride.chem.msu.ru*

Received January 17, 2020; revised June 29, 2020; accepted June 30, 2020

Abstract—We have synthesized $(ZrTi)_{0.5}(VCrFe(Ni_{0.9}Cu_{0.1}))_{0.5}$ and $(ZrTi)_{0.5}(VMoFeNi)_{0.5}$ pseudobinary high-entropy compounds and related deuterides. According to neutron and X-ray diffraction results, the deuterides have the same hexagonal Laves phase structure as the parent alloys. We have determined the position of the deuterium atoms and their atomic position coordinates. The results indicate that the deuterium atoms reside predominantly in positions 24*l* and 12k_2, typical of hydrogen in hexagonal Laves phases.

Keywords: high-entropy compounds, deuterides, neutron diffraction

DOI: 10.1134/S0020168520110138

INTRODUCTION

High-entropy alloys possess unique properties [1, 2], including good high-temperature strength, high corrosion resistance, increased wear resistance, and good mechanical strength. Such materials are always highly demanded in industry for the manufacture of cutting tools, in mechanisms containing dry friction pairs, and in powder metallurgy for the manufacture of articles.

The compounds studied in this work, $(ZrTi)_{0.5}(VCrFe(Ni_{0.9}Cu_{0.1}))_{0.5}$ and $(ZrTi)_{0.5}(VMoFeNi)_{0.5}$, have the hexagonal Laves phase structure *C*14 (*C*14: $MgZn_2$ structure; *C*15: $MgCu_2$ structure; *C*36: $MgNi_2$ structure). It is known that, in many cases, compounds with a Laves phase structure reversibly absorb considerable amounts of hydrogen and can be used as hydrogen storage materials [3, 4].

In recent years, intensive research effort has been concentrated on reactions of high-entropy compounds with hydrogen. For example, Kunce et al. [5] studied reaction of a ZrTiVCrFeNi high-entropy alloy with hydrogen. Measured hydrogen absorption–desorption isotherms showed that the system contained a hydride phase with 2.2 hydrogen atoms per formula unit (FU) of the intermetallic compound (2.2 H/FU). According to X-ray diffraction data, the hydride had an expanded lattice with the Laves phase structure *C*14. The relative increase in the unit-cell volume of the hydride ($\Delta V/V$) was determined to be 23%. Kao et al. [6] investigated interaction of hydrogen with a series of TiZrVCoFeMn-based high-entropy alloys with the hexagonal Laves phase structure *C*14. They varied the percentages of Ti, Zr, and V. Measured hydrogen absorption–desorption isotherms indicated the formation of hydride phases for some of the alloys, in which the highest hydrogen content was 2.2 H/FU. Chen et al. [7] studied hydrogen sorption properties of TiZrVFeMnCr-based high-entropy alloys, sequentially substituting titanium for zirconium and also manganese for iron, chromium, and vanadium, so that the alloys retained the *C*14 structure. They measured hydrogen desorption isotherms for all of the compounds thus obtained and determined thermodynamic parameters of the decomposition of the hydride phases. According to X-ray diffraction data, the synthesized hydrides had an expanded lattice with the Laves phase structure *C*14. The highest hydrogen content of the synthesized hydride phases was 2.1 H/FU.

One structural feature of the $(ZrTi)_{0.5}(VCrFe(Ni_{0.9}Cu_{0.1}))_{0.5}$ and $(ZrTi)_{0.5}(VMoFeNi)_{0.5}$ compounds is a random atom distribution over their lattice sites. Because of this, unlike in the case of well-studied hydrides, for example, those based on the ZrVCo compound [8], the structure of the metallic matrix of these compounds was refined using a tentative distribution of the metal atoms over crystallographic sites. This approach is known in the literature and is usually utilized in determining the structure of deuterided multicomponent alloys by X-ray and neutron diffraction techniques [9, 10].

The objectives of this work were to study the structure of deuterides based on high-entropy alloys, determine structural parameters of the deuterium atoms, and compare the structure of these compounds to

Table 1. Unit-cell parameters of the intermetallic compounds and related deuterides

Composition	a, nm	c, nm	V, nm$^3 \times 10^{-3}$	$\Delta V/V$, %
$(ZrTi)_{0.5}(VCrFe(Ni_{0.9}Cu_{0.1}))_{0.5}$	0.4972(2)	0.8120(1)	17.4	–
$(ZrTi)_{0.5}(VCrFe(Ni_{0.9}Cu_{0.1}))_{0.5}D_{2.5}$	0.5235(2)	0.8550(3)	20.3	17.0
$(ZrTi)_{0.5}(VMoFeNi)_{0.5}$	0.4916(2)	0.8030(2)	17.2	–
$(ZrTi)_{0.5}(VMoFeNi)_{0.5}D_{3.0}$	0.5321(2)	0.8680(2)	21.3	23.0

those reported in the literature. The structure of the metallic matrix was refined using both neutron diffraction measurements and X-ray diffraction data.

EXPERIMENTAL

The $(ZrTi)_{0.5}(VCrFe(Ni_{0.9}Cu_{0.1}))_{0.5}$ and $(ZrTi)_{0.5}(VMoFeNi)_{0.5}$ alloys were prepared by electric arc melting of pure metals in an inert atmosphere and annealed for 240 h at a temperature of 1073 K in a quartz ampule sealed under vacuum. Deuterides were synthesized in a Sieverts apparatus with hydrogen pressures of up to 10 MPa. The amount of deuterium in the synthesized deuterides was evaluated by a volumetric technique using the van der Waals equation for real gases. To prevent deuterium losses, the synthesized deuteride samples were passivated by cooling in liquid nitrogen and holding in air [11].

The alloys and deuterides were characterized by X-ray diffraction on a ThermoARL diffractometer (Cu target X-ray tube). Neutron diffraction measurements were made at room temperature at the ATOS station of the IR-8 reactor at the Kurchatov Institute (National Research Centre). The results were analyzed by the Rietveld method using FullProf and Rietan software.

RESULTS AND DISCUSSION

X-ray diffraction characterization showed that the synthesized $(ZrTi)_{0.5}(VCrFe(Ni_{0.9}Cu_{0.1}))_{0.5}$ and $(ZrTi)_{0.5}(VMoFeNi)_{0.5}$ samples were single-phase and had the hexagonal Laves phase structure $C14$ (Table 1; Figs. 1, 2). In refining the X-ray diffraction data, the chemical compositions of the samples were taken to be $(ZrTi)_{0.5}(VCrFe(Ni_{0.9}Cu_{0.1}))_{0.5}$ and $(ZrTi)_{0.5}(VMoFeNi)_{0.5}$. These compositions correspond to the quantitative content of components in an AB_2 Laves phase with a $C14$ hexagonal lattice.

After interaction with deuterium, the $(ZrTi)_{0.5}(VCrFe(Ni_{0.9}Cu_{0.1}))_{0.5}$ and $(ZrTi)_{0.5}(VMoFeNi)_{0.5}$ samples contained 2.5 and 3.0 D/FU, respectively, at a deuterium pressure of 1.5 MPa and room temperature. X-ray diffraction characterization of the passivated deuteride samples showed that their lattice was expanded and retained the $C14$ hexagonal structure of the parent compounds (Table 1; Figs 3, 4).

In determining the structure of the samples under study, we took into account the multicomponent composition of the metallic matrix of the deuterides. Its characteristic feature is that atoms similar in number are almost indistinguishable for X-ray rays. In the case of neutron diffraction measurements, vanadium atoms are essentially "invisible." In previously reported structural studies of Laves phases of similar multicomponent compounds, it is commonly assumed that the large metallic atoms are randomly distributed over position 4*f* of component A, whereas the smaller atoms occupy positions 2*a* and 6*h* in the B sublattice [10, 12]. In our case, we also think that the large atoms (Zr and Ti) occupy position 4*f* in the structure of the alloys. The smaller atoms (V, Cr, Fe, Ni, Cu, and Mo) occupy positions 2*a* and 6*h*. In neutron diffraction data processing (Figs. 5, 6; Tables 2, 3), we refined only structural parameters of the deuterium atoms. The refinement results demonstrate that the deuterium atoms occupy predominantly two types of position: 24*l* and $12k_2$. Positions $6h_1$ and $6h_2$ have insignificant occupancies. Note that the ratio of the occupancies of positions 24*l* and $12k_2$ is about 2 : 1.

This occupancy ratio indicates that, the filling of these positions with deuterium atoms does not ensure stoichiometry and that there is no complete deuterium ordering in these positions. The same is evidenced by the present experimental data: the neutron diffraction patterns of the deuterides (Figs. 5, 6) contain a weak halo, indicative that the deuterium is in a disordered state.

As shown earlier for well-studied transition metal hydrides [13, 14] and intermetallic hydrides [15, 16], such a sequential filling of structural sites is due to a short-range order ("blocking") in the arrangement of the hydrogen atoms. According to previously reported experimental data [14–16], "blocking" is determined by a radius which is on average 0.2 nm and varies from 0.18 to 0.22 nm in different hydrides. This radius depends on the lattice parameters of the alloy or intermetallic phase, the positional parameters in its structure, and hydrogen content. Note that the presence of deuterium in a single sublattice is only likely at large "blocking" radii, small lattice parameters, and low hydrogen concentration. Otherwise, deuterium occupies positions in many sublattices of the metallic matrix of the deuterides. The present experimental data on site occupancies con-

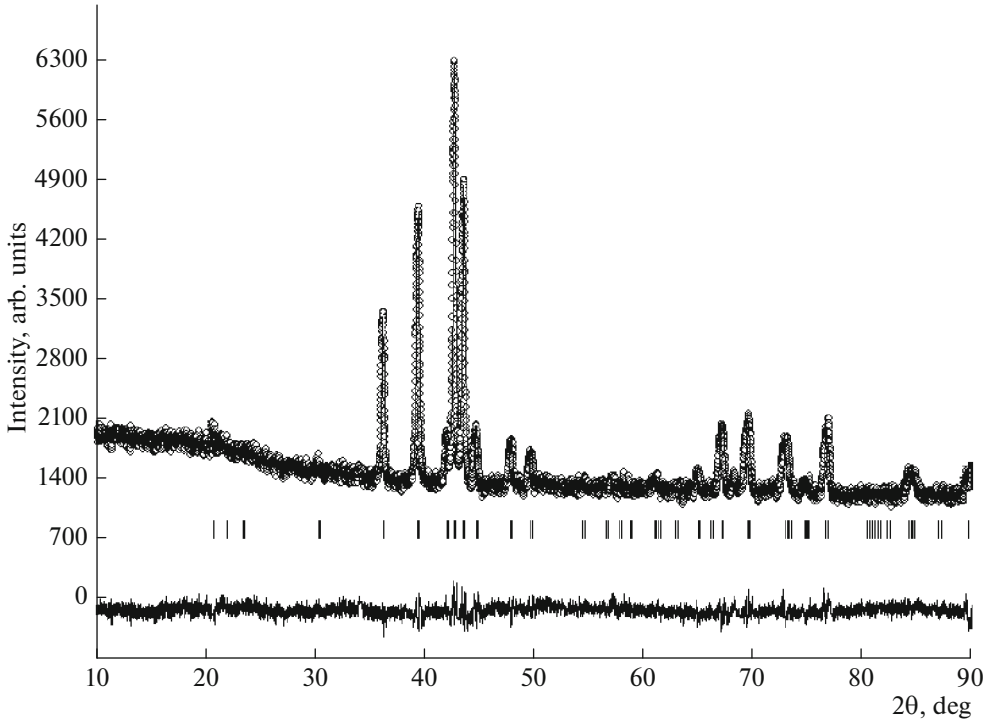

Fig. 1. Rietveld refinement profile for the $(ZrTi)_{0.5}(VCrFe(Ni_{0.9}Cu_{0.1}))_{0.5}$ alloy: the open circles represent the raw X-ray diffraction data, the upper continuous line is the calculated profile, and the lower continuous line is the difference plot. The vertical tick marks show the positions of Bragg reflections.

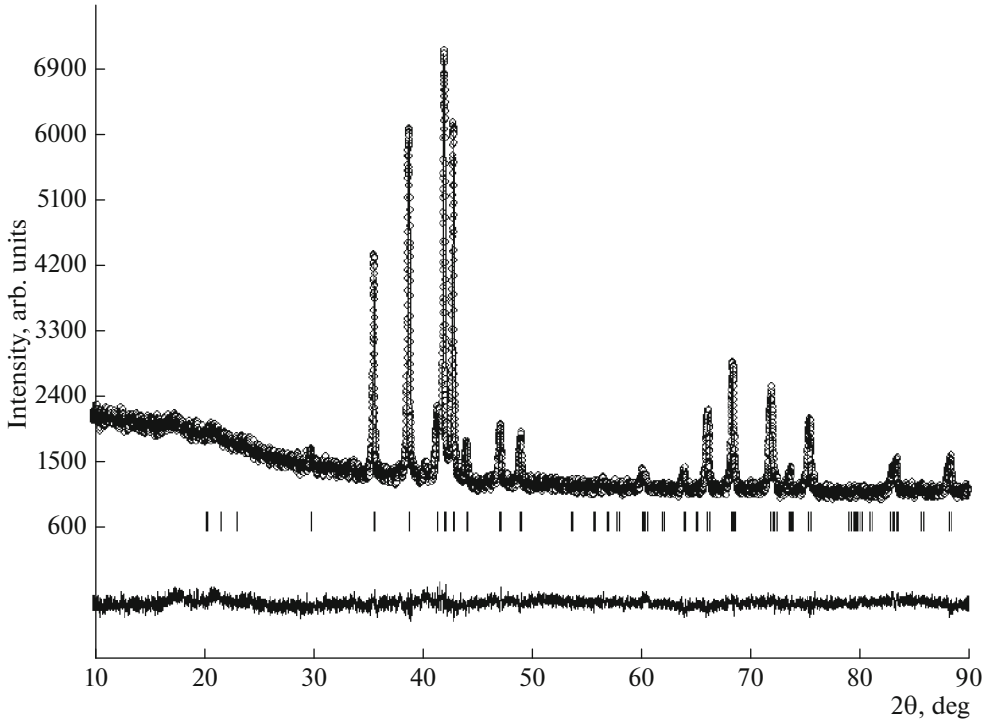

Fig. 2. Rietveld refinement profile for the $(ZrTi)_{0.5}(VMoFeNi)_{0.5}$ alloy.

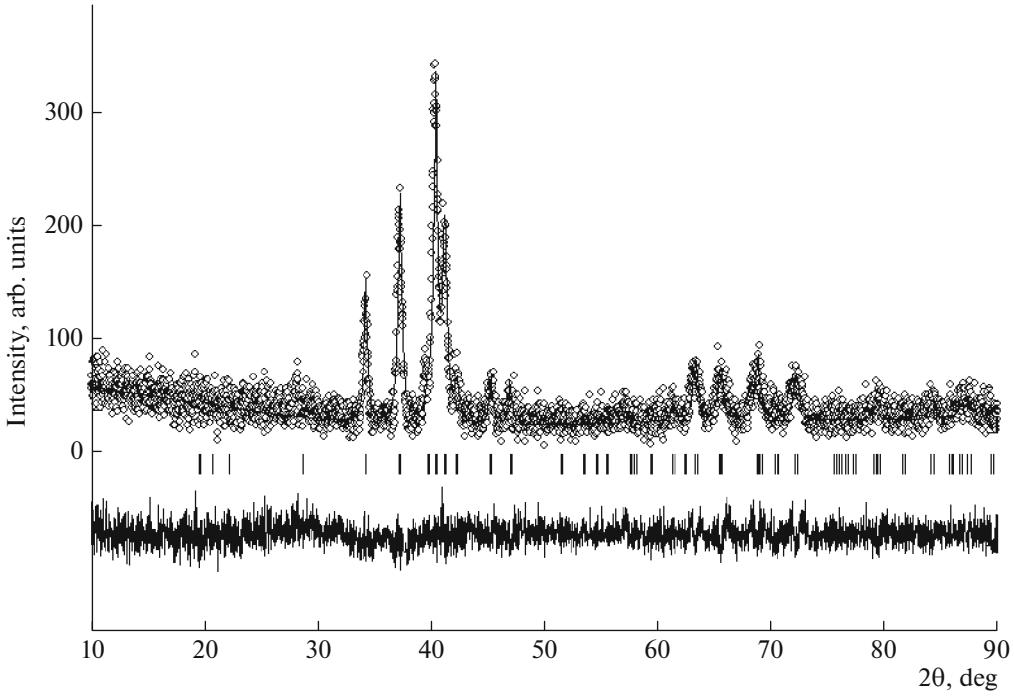

Fig. 3. Rietveld refinement profile for the $(ZrTi)_{0.5}(VCrFe(Ni_{0.9}Cu_{0.1}))_{0.5}D_{2.5}$ deuteride.

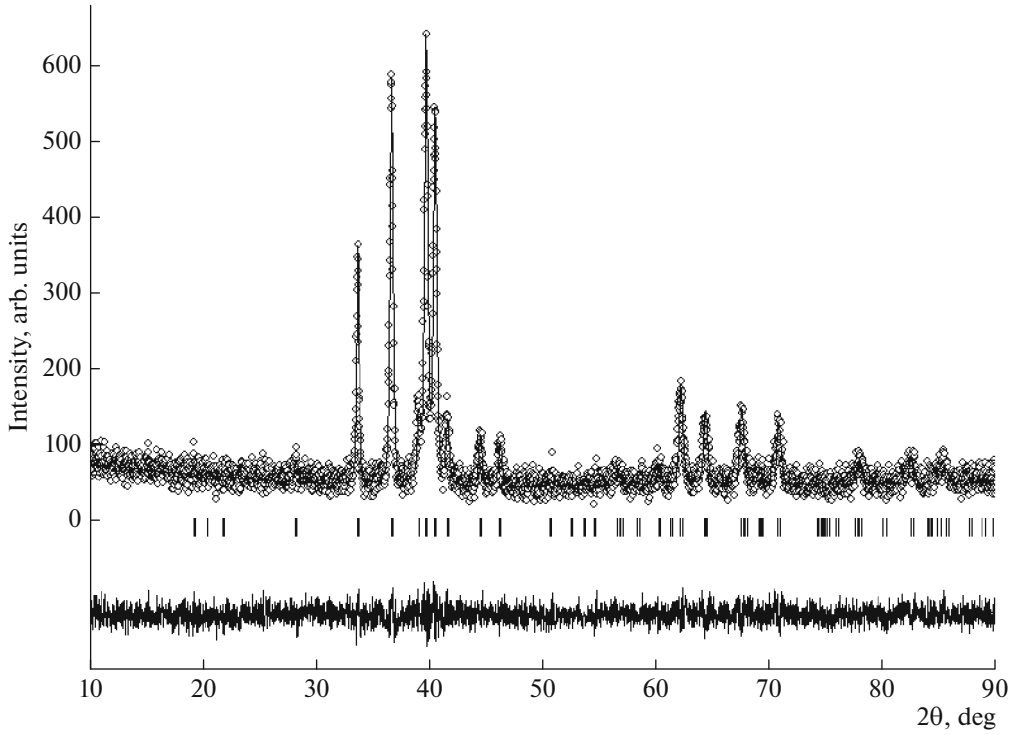

Fig. 4. Rietveld refinement profile for the $(ZrTi)_{0.5}(VMoFeNi)_{0.5}D_{3.0}$ deuteride.

firm that the "blocking" effect influences the distribution of deuterium atoms over the metallic sublattice of the $(ZrTi)_{0.5}(VCrFe(Ni_{0.9}Cu_{0.1}))_{0.5}D_{2.5}$ and $(ZrTi)_{0.5}(VMoFeNi)_{0.5}D_{3.0}$ deuterides.

Comparison of the deuterides studied in this work with the ZrVCO-based deuterides investigated by Souberoux et al. [8] demonstrates a similar deuterium distribution. The deuterium in the ZrVCo-based deu-

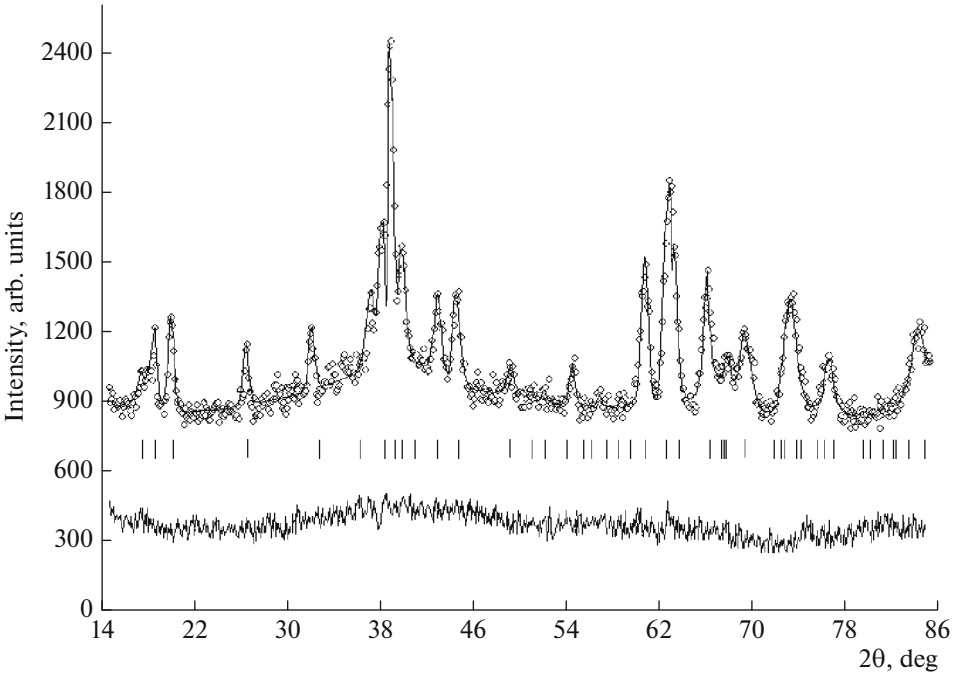

Fig. 5. Rietveld refinement profile for the $(ZrTi)_{0.5}(VCrFe(Ni_{0.9}Cu_{0.1}))_{0.5}D_{2.5}$ deuteride: the open circles represent the raw neutron diffraction data, the upper continuous line is the calculated profile, and the lower continuous line is the difference plot. The vertical tick marks show the positions of the Bragg reflections from the deuteride phase ($R_w = 7.0\%$).

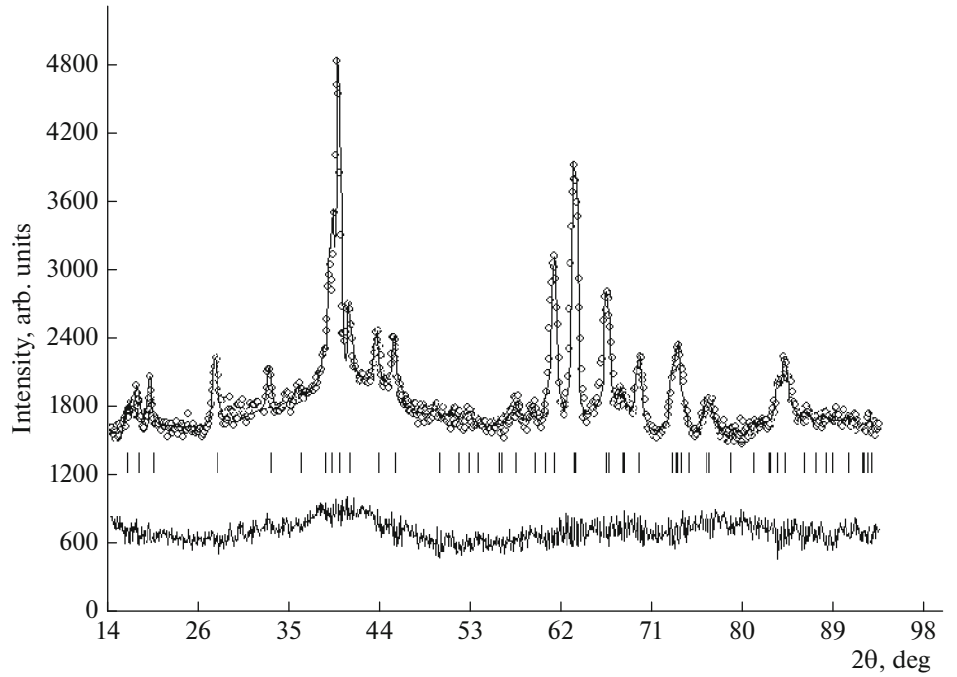

Fig. 6. Rietveld refinement profile for the $(ZrTi)_{0.5}(VMoFeNi)_{0.5}D_{3.0}$ deuteride: the open circles represent the raw neutron diffraction data, the upper continuous line is the calculated profile, and the lower continuous line is the difference plot. The vertical tick marks show the positions of the Bragg reflections from the deuteride phase ($R_w = 7.6\%$).

terides was shown to reside in positions whose occupancies decrease in the sequence $24l > 12k_2 > 6h_1 > 6h_2$. In our case, the occupancies of the two most occupied positions, $24l$ and $12k_2$, are also observed to decrease. The bond distances in the deuterides studied here (Table 3) approach those in the deuterides stud-

Table 2. Structural data for the deuterides

Atoms	Position	Site occupancy	Atomic coordinates		
			x	*y*	*z*
$(ZrTi)_{0.5}(VCrFe(Ni_{0.9}Cu_{0.1}))_{0.5}D_{2.5}$					
Zr,Ti	4*f*	1.0	0.333	0.666	0.085(2)
Cr, Fe, Ni, Cu	2*a*	1.0	0	0	0
Cr, Fe, Ni, Cu	6*h*	1.0	0.833(2)	0.666(2)	0.25
D1	24*l*	0.33(2)	0.040(3)	0.328(3)	0.551(2)
D2	$12k_2$	0.17(1)	0.430(2)	0.882(2)	0.621(3)
$(ZrTi)_{0.5}(VMoFeNi)_{0.5}D_{3.0}$					
Zr,Ti	4*f*	1.0	0.333	0.666	0.087(3)
Mo, Fe, Ni	2*a*	1.0	0	0	0
Mo, Fe, Ni	6*h*	1.0	0.833(1)	0.666(1)	0.25
D1	24*l*	0.39(2)	0.039(2)	0.327(2)	0.554(3)
D2	$12k_2$	0.22(2)	0.467(3)	0.891(3)	0.633(2)

Table 3. Bond distances in the deuterides

Atoms	*d*, nm	Atoms	*d*, nm
$(ZrTi)_{0.5}(VCrFe(Ni_{0.9}Cu_{0.1}))_{0.5}D_{2.5}$			
(Zr,Ti)–(Zr,Ti)	0.319	(V, Cr, Fe, Ni,Cu)–D1	0.178
(Zr,Ti)–(V, Cr, F e, Ni, Cu)	0.306	(V, Cr, Fe, Ni,Cu)–D2	0.179
(V, Cr,Fe, Ni,Cu)–(V, Cr, Fe, Ni, Cu)	0.261	D1–D1	0.215
(Zr,Ti)–D1	0.193	D2–D2	0.206
(Zr,Ti)–D2	0.190		
$(ZrTi)_{0.5}(VMoFeNi)_{0.5}D_{3.0}$			
(Zr,Ti)–(Zr,Ti)	0.324	(V, Mo, Fe, Ni)–D1	0.178
(Zr,Ti)–(V, Mo, Fe, Ni)	0.311	(V, Mo, Fe, Ni)–D2	0.180
(Mo, Fe, Ni)–(V, Mo, Fe, Ni)	0.266	D1-D2	0.202
(Zr,Ti)–D1	0.194	D1-D2	0.210
(Zr,Ti)–D2	0.189		

ied by Souberoux et al. [8] and having similar hydrogen concentration [8]. The bond distances in these deuterides can be evaluated from the structural data obtained in this study.

CONCLUSIONS

We have synthesized deuterides based on high-entropy compounds with the hexagonal Laves phase structure *C*14 and the compositions $(ZrTi)_{0.5}(VCrFe(Ni_{0.9}Cu_{0.1}))_{0.5}D_{2.5}$ and $(ZrTi)_{0.5}(VMoFeNi)_{0.5}D_{3.0}$. The structure of the synthesized deuterides has been studied by X-ray and neutron diffraction techniques. The results indicate that the deuterium atoms reside predominantly in positions 24*l* and $12k_2$ in the ratio 2 : 1, differing from the stoichiometric one. These site occupancies are interpreted in terms of the notion of complete or partial site "blocking" by deuterium atoms, characteristic of previously studied hydrides.

REFERENCES

1. Miracle, D.B. and Senkov, O.N., A critical review of high entropy alloys and related concepts, *Acta Mater.,* 2017, vol. 122, pp. 448–511.

2. Xu, Z.Q., Ma, Z.L., Wang, M., Chen, Y.W., Tan, Y.D., and Cheng, X.W., Design of novel low-density refractory high entropy alloys for high-temperature applications, *Mater. Sci. Eng.: A,* 2019, vol. 755, no. 7, pp. 925–931.

3. Sandrock, G., A panoramic overview of hydrogen storage alloys from a gas reaction point of view, *J. Alloys Compd.,* 1999, vol. 293-295, pp. 877–888.

4. Verbetsky, V.N. and Mitrokhin, S.V., Properties and potential applications of metal hydrides, *Materialovedenie,* 2009, no. 1, pp. 48–60.

5. Kunce, I., Polanski, M., and Bystrzycki, J., Structure and hydrogen storage properties of a high entropy ZrTiVCrFeNi alloy synthesized using laser engineered net shaping (LENS), *Int. J. Hydrogen Energy,* 2013, vol. 38, pp. 12180–12189.

6. Kao, Y.F., Chen, S.K., Sheu, J.H., et al., Hydrogen storage properties of multi-principal-component $CoFeMnTi_xV_yZr_z$ alloys, *Int. J. Hydrogen Energy,* 2010, vol. 35, pp. 9056–9059.

7. Chen, S.K. Lee, P.H., et al., Hydrogen storage of *C*-14 $Cr_uFe_vMn_wTi_xV_yZr_z$ alloys, *Mater. Chem. Phys.,* 2018, vol. 210, pp. 336–347.

8. Souberoux, J.L., Fruchart, D., and Biris, A.S., Structural studies of Laves phases $ZrVCo(V_{1-x}Cr_x)$ with $0 < x < 1$ and their hydrides, *J. Alloys Compd.,* 1999, vols. 293–295, pp. 88–92.

9. Yartys, V.A., Burnasheva, V.V., Fadeeva, N.V., Solovjev, S.P., and Semenenko, K.N., Crystal chemistry of $RT_5H(D)_x$, $RT_2H(D)_x$ and $RT_3H(D)_x$ hydrides based on intermetallic compounds of $CaCu_5$, $MgCu_2$, $MgZn_2$ and $PuNi_3$ structure types, *Int. J. Hydrogen Energy,* 1982, vol. 7, pp. 957–965.

10. Didisheim, J.J., Yvon, K., Shaltiel, D., and Fisher, P., The distribution of the deuterium atoms in the deuterated hexagonal Laves-phase $ZrMn_2D_3$, *Solid State Commun.,* 1979, vol. 31, pp. 47–50.

11. Lushnikov, S.A., Verbetsky, V.N., Glazkov, V.P., and Somenkov, V.A., Structure of deuterided NbVCo, *Inorg. Mater.,* 2006, vol. 42, no. 7, pp. 771–776.

12. Triantatillidis, G., Pontonnier, L., Fruchart, D., Wolfers, P., and Souberoux, J., Effect of hydrogen absorption on the structural properties of the hyperstoichiometric alloys $Zr(Mn_{0.72}Fe_{0.28})_{2+x}$, *J. Less-Common Met.,* 1991, vols. 172–174, pp. 183–190.

13. Somenkov, V.A., Structure of hydrides, *Ber. Bunsen-Ges. Phys. Chem.,* 1972, vol. 76, pp. 724–728.

14. Somenkov, V.A. and Shilstein, S.Sh., Phase transition of hydrogen in metals, *Prog. Mater. Sci.,* 1979, vol. 24, pp. 267–269.

15. Irodova, A.V., Orientation ordering ($k = 0$) in solid solutions of hydrogen in cubic (*C*15) Laves phases, *Preprint of Kurchatov Inst. of Atomic Energy,* Moscow, 1980, no. 3308/9, pp. 1–16.

16. Scripov, A.V., Hydrogen jump motion in Laves-phase hydrides: two frequency scales, *Int. Symp. on Metal–Hydrogen Systems,* Crakow, 2004.

Translated by O. Tsarev